Response kinetics in the complex chemotaxis signalling pathway of Rhodobacter sphaeroides

Article

Accepted Version

Response kinetics in the complex chemotaxis signalling pathway of *Rhodobacter sphaeroides*

Mila Kojadinovic[1♣], Judith P. Armitage[1], Marcus J. Tindall[2,3,4] and George H. Wadhams[1*].

[1] Oxford Centre for Integrative Systems Biology, Department of Biochemistry, University of Oxford, South Parks Road, Oxford, OX1 3QU, U.K.

[2] Department of Mathematics and Statistics, University of Reading, Whiteknights, PO Box 220, Reading, RG6 6AX, U.K.

[3] School of Biological Sciences, University of Reading, Whiteknights, Reading, RG6 6BX, U.K.

[4] Institute for Cardiovascular and Metabolic Research, University of Reading, Whiteknights, PO Box 218, Reading, RG6 6AA. U.K.

*For correspondence. E-mail: george.wadhams@bioch.ox.ac.uk; Tel. (+44) 1865 613329; Fax. (+44) 1865 613338.

♣Present address: Department of Zoology, University of Oxford, South Parks Road, Oxford, OX1 3PS, U. K.

Keywords: Chemotaxis, Weber's law, Fold-Change Detection, Response kinetics, *Rhodobacter sphaeroides*.

SUMMARY

Chemotaxis is one of the best characterised signalling systems in biology. It is the mechanism by which bacteria move towards optimal environments and is implicated in biofilm formation, pathogenesis and symbiosis. The properties of the bacterial chemosensory response have been described in detail for the single chemosensory pathway of *Escherichia coli*. We have characterised the properties of the chemosensory response of *Rhodobacter sphaeroides,* an α-proteobacterium with multiple chemotaxis pathways, under two growth conditions allowing the effects of protein expression levels and cell architecture to be investigated. Using tethered cell assays we measured the responses of the system to step changes in concentration of the attractant propionate and show that, independently of the growth conditions, *R. sphaeroides* is chemotactic over at least five orders of magnitude and has a sensing profile following Weber's law. Mathematical modelling also shows that, like *E. coli*, *R. sphaeroides* is capable of showing Fold-Change Detection (FCD). Our results indicate that general features of bacterial chemotaxis such as the range and sensitivity of detection, adaptation times, adherence to Weber's law and the presence of FCD may be integral features of chemotaxis systems in general, regardless of network complexity, protein expression levels and cellular architecture across different species.

1. INTRODUCTION

Chemotaxis allows swimming bacteria to move towards optimal environments for growth by performing temporal comparisons of chemoeffector concentrations [1,2]. For decades the chemosensory system has been used as a paradigm for bacterial signalling systems and has been extensively studied both experimentally and via the use of mathematical modelling. Although chemotaxis is widespread among bacterial species and central to establishment of symbioses [3,4,5], biofilm formation [6] and virulence [7,8], the processes and features of chemosensory signalling have been principally investigated in *Escherichia coli* [9]. This study investigates whether the underlying principles elucidated for *E. coli* hold for chemosensory systems in other species, especially those with more complex internal signalling networks.

Most bacteria swim by rotating semi-rigid, helical flagella and change direction every few seconds [10]. These changes are due to transient reversals in the direction of flagellar motor rotation causing tumbles during which bacteria are reorientated. When swimming resumes it is generally in a new direction, resulting in the bacteria moving in a random walk [11]. In non-homogeneous environments, modulation of the tumbling frequency by the chemotaxis signalling pathway biases the overall bacterial movement in a favourable direction. *E. coli* has a single chemotaxis signalling pathway, reviewed in [9,12,13,14]. Transmembrane receptors sense changes in chemoeffector concentrations and the signal is relayed to the flagellar motor through a diffusible phosphorylatable protein, CheY. Cells adapt to the persistence of the signal by methylation/demethylation of the receptors, returning behaviour to its pre-stimulus pattern. The *E. coli* sensory system is extremely sensitive, detecting changes as low as 3 nM aspartate [15] and able to respond to changes in chemoeffector concentration over five to six orders in magnitude [10,16,17]. This system has been shown to sense relative changes in chemoeffector concentration and not absolute changes, behaviour thought to conform to Weber's law [16,18].

Recent work performed by Lazova and colleagues [19] has demonstrated not only that *E. coli* chemotaxis follows Weber's law, but that it also shows Fold-Change Detection (FCD) as predicted by Shoval *et al.* [20]. FCD encompasses Weber's law but it is more exacting. For a sensory system displaying FCD, the entire shape of the response must be identical for fold-changes in chemoeffector concentration i.e. responses to identical fold-changes show equal amplitudes and adaptation times, and a steady post stimulus state identical to the pre-stimulus state, known as exact adaptation [19,20]. Our current study investigates whether these properties are specific to the single chemotaxis pathway in *E. coli* or are also observed in other, more complex, chemotaxis systems.

R. sphaeroides is a purple non-sulfur α-proteobacterium able to grow using either aerobic or anaerobic respiration or photosynthesis and shows taxis to a wide range of stimuli including sugars, light, oxygen and organic acids such as propionate [21,22,23]. Interestingly, this bacterium is able to tune its tactic responses to the environmental conditions with responses to certain stimuli such as oxygen and light depending on growth conditions [24,25,26]. It has a number of differences in its chemosensory pathway when compared to *E. coli* (figure S1). A comparison of the response characteristics of the two species will suggest how universal the input:output function of chemosensory systems is across species. Unlike *E. coli* with a single chemosensory pathway *R. sphaeroides* expresses two pathways under laboratory conditions [22,23]. The proteins of one chemosensory pathway localise with membrane spanning receptors at the cell poles, sensing the extracellular environment, while those of a second pathway localise with soluble chemoreceptors in a cluster in the cytoplasm, sensing the intracellular environment. Signals from the two pathways, in the form of CheY-Ps, must balance to control the behaviour of a single flagellar motor, and this study is aimed at identifying whether the input:output

relationship from this complex two chemosensory pathway system is similar to that from a more simple single chemosensory pathway.

Aerobically and photoheterotrophically grown *R. sphaeroides* cells also have different cell architecture, with the membrane invaginating extensively under photosynthetic conditions to accommodate the photosynthetic complexes [27], possibly altering diffusion rates and interfering with chemosensory signalling. Under these different growth conditions, whilst both pathways are expressed, the expression levels of the two pathways alters [28,29] and while both types of cell show chemotaxis it is possible that their input:output characteristics might differ.

In the present study, using tethered cell assays, we have measured the chemotactic responses of individual aerobically and photosynthetically grown cells to a range of step decreases in propionate concentration. Our results indicate that, independently of the growth conditions, *R. sphaeroides* is chemotactic over at least five orders of magnitude, can sense changes in concentration as low as 10 nM and has a sensing profile following Weber's law. We demonstrate that, irrespective of the growth conditions and despite variability between cells in terms of adaptation times and responsiveness to stimuli, our experimental data are consistent with *R. sphaeroides* showing Fold-Change Detection and mathematical modelling of this complex signalling pathway supports the fact that it is capable of demonstrating FCD. These data suggest that chemosensory stimuli sensed through two physically separate pathways, in cells with different cellular architectures, balance to produce an output response with the same characteristics as the output from the single well characterised pathway of *E. coli*. In conjunction with other modelling data [30], this supports the notion that the underlying features of the chemosensory signalling system may be universal amongst diverse bacterial species.

2. METHODS

2.1. Growth conditions

R. sphaeroides WS8N [31] was grown in succinate medium [32] at 30°C either aerobically in the dark in 250 ml flasks containing 50 ml of medium shaken at 255 rpm or photoheterotrophic without shaking, in airtight 25 ml flasks illuminated with white light at low intensity ($5W/m^2$) to maximise membrane invaginations. Cells were harvested at mid-exponential phase (OD_{700} between 0.45 and 0.55) when cells are very motile. This also ensures limited self-shading in photosynthetic conditions and oxygen saturation for aerobic cultures.

2.2. Cell tethering and motion analysis

One millilitre of cells in mid-exponential phase was harvested, washed and resuspended in tethering buffer (10 mM Na-PIPES, containing chloramphenicol at 30 µg ml^{-1} to stop protein synthesis). Cells were tethered by their flagella onto a coverslip by adding 10 µl of cell suspension with 2 µl of 10,000X diluted anti-flagella antibody which spontaneously adsorb to the coverslip glass. The coverslip was incubated for 20 minutes in a humidity chamber and was then inverted onto a microscope flow chamber and tethering buffer or propionate solutions successively flowed through at a rate of 0.12 ml min^{-1} during 5 minute sequences. Cells were observed and recorded using 40X magnification under phase contrast (Nikon Optiphot phase contrast Microscope). Tethered cells were recorded using a digital DALSA Genie-HM640 camera with an acquisition frame rate of 100 fps and an exposure time of 6 ms. Movies were analysed using software BRAS and rotation speeds of single-bacteria extracted and analyzed using the graphical interface “click & mean” [33]. For each type of experiment and each type of cells studied, at least three biological replicates were analysed.

2.3. Data analysis

Tethered cells were divided into two categories; unresponsive cells, showing no stop within two minutes of a reduction in propionate concentration, and responsive cells showing a stop within this timeframe. The percentage of cells responding to a given stimulus was calculated from the total number of responsive and unresponsive cells obtained from experiments across at least three biological replicates. The general responses of single-cells or populations and the variations within responses were determined from at least three measurements by calculating data medians and Interquartile Ranges (IQRs: defined as the difference between the third and the first quartiles of the data) respectively.

3. RESULTS

3.1. Population responses conform to Weber's law

To determine the range of propionate concentrations over which *R. sphaeroides* is chemotactic and the sensitivity of *R. sphaeroides* chemosensory system, we measured the chemosensory responses of tethered cells to reductions in concentration ranging over 5 orders of magnitude. Cells were successively challenged with six different stimuli (10 nM to zero, 100 nM to zero, 1 µM to zero, 10 µM to zero, 100 µM to zero and 1 mM to zero) and their responses measured. As illustrated in figure 1*a*, a proportion of cells grown under either aerobic or photosynthetic conditions are sensitive to changes in propionate over at least 5 orders of magnitude. For both growth conditions, the majority of the cells (more than 50%) react to drops greater than 10 µM, with fewer cells responding to lower concentrations drops (figure 1*a*). The increase in the percentage of aerobically grown cells responding to a drop from 10nM to zero is probably due to intrinsic cell to cell variation (see section 3.2) coupled with the low number of cells responding to these concentrations.

We then investigated whether *R. sphaeroides* reacts to absolute or relative changes in attractant concentration. As over 50 % of cells react to steps down in propionate concentration of between 1 mM and 10 µM to zero, we tested how an identical 10 µM drop in propionate concentration is sensed over different background concentrations ranging from 1 mM to 10 µM. We successively challenged cells with the following stimuli: 1010 µM to 1000 µM, 1000 µM to 110 µM, 110 µM to 100 µM, 100 µM to 20 µM, 20 µM to 10 µM and 10 µM to zero. This enabled us to alternate between 10 µM absolute drops in propionate concentration, corresponding to low relative changes in propionate concentration, and to high relative changes in propionate concentration. Figure 1*b* demonstrates that, in both aerobically and photosynthetically grown cells, 10 µM drops are poorly detected against high background concentrations while changes of 5-fold or greater trigger responses in a significant percentage of cells. *R. sphaeroides* therefore appears to sense relative and not absolute changes in attractant concentration. Interestingly, the percentages of responsive cells were generally higher for aerobically grown cells than for photosynthetically grown cells (figure 1*b*).

Since our results showed that a significant percentage of cells react to a 5-fold drop in concentration we tested responses to 5-fold drops in propionate concentration over background concentrations ranging from 12.5 mM to 4 µM. Our results indicate that a significant percentage of cells react to 5-fold drops in propionate over a background range of 0.5 mM to 4 µM concentration (figure 1*c*). However, for background concentrations over 0.5 mM, the percentages of responsive cells decrease, dropping to less than 50 % for aerobic cells and almost zero for photosynthetic cells (figure 1*c*). Therefore, within a specific range of background concentrations and irrespective of the growth conditions, the cells react similarly to 5-fold drops. This shows that

R. sphaeroides reacts to relative changes in concentrations, and thus the responses follow Weber's law.

3.2. Single- cell analysis of adaptation times

An intriguing feature of *E. coli* chemotaxis is that the intracellular signalling pathway not only obeys Weber's law, but also shows FCD [19]. As our results suggested that *R. sphaeroides* sensing follows Weber's law, we investigated whether FCD could also be a feature of *R. sphaeroides* chemosensing. In order to test this hypothesis, we analyzed the adaptation times (the time taken to return to the pre-stimulus rotation pattern in the continued presence of the stimulus) of individual cells within the population to different 5-fold drops over background concentration between 12.5 mM and 4 µM. In addition, we challenged bacteria with six identical 5-fold drops (from 100 µM propionate to 20 µM) to determine the intrinsic variability in *R. sphaeroides* chemosensory responses in terms of adaptation time.

Analysis of the responses of single cells reacting to six repeated challenges with identical 5-fold drops (from 100 µM propionate to 20 µM) showed a degree of underlying intrinsic cell to cell variability in their response times (figure 2*a*, *b* and S2) consistent with that seen in other systems [34,35,36]. However, comparing these data to those obtained after challenging cells with different 5-fold drops over background concentration between 12.5 mM and 4 µM, the variations in response times for single-cells challenged multiple times with different stimuli showed no significant difference to the intrinsic variations in adaptation times (figure 2 and S2, Kruskal-Wallis rank sum test, p-value > 0.05). Combining these single cell responses to look at the median adaptation time for each population shows that, irrespective of the growth conditions, the variability observed in population adaptation times to different 5-fold drops is similar to the basal response variability of *R. sphaeroides* populations (figure 3 and S3). Interestingly, despite

differences in protein copy number and cellular morphology, both photosynthetic and aerobic cell populations show similar adaptation times to 5-fold drops in concentration (figure 3*a* and 3*b*). Thus, these data show that, independently of the growth conditions, *R. sphaeroides* cells have similar chemotactic responses which are consistent with the requirements for FCD.

3.3. Can the R. sphaeroides *chemosensory pathway show true FCD?*

A fundamental feature of FCD is that the entire shape of the chemosensory response (amplitude, adaptation time and precision of return to prestimulus behaviour) must be identical for the same fold changes in input [20]. Due to the large number of proteins within the complex chemotaxis system of *R. sphaeroides* it is not possible to experimentally measure the amplitudes and dynamics of all of the components of the system. Therefore, to determine whether the chemosensory pathway of *R. sphaeroides* is capable of showing true FCD we developed a nonlinear ODE model to characterise the changes in the intracellular signalling pathway components on different 5-fold drops in attractant concentration. The mathematical model was formulated around earlier simpler models of the *R. sphaeroides* signaling cascade [37], but which did not include a model of adaptation. As such we integrated a recent Monod-Wyman-Changeux (MWC) model of *E. coli* receptor adaptation [38] with the underlying *R. sphaeroides* signaling cascade in a similar manner to that of Clausznitzer *et al.* [39] for *E. coli* chemotaxis. Full details of the mathematical model and its parameter values are given in the Supplementary Information. This mathematical model is similar in features to that of Tu *et al.* [40], which exhibited FCD under specific conditions [20] and satisfies the conditions that are shown by Hamadeh and colleagues to be sufficient for the *R. sphaeroides* chemotaxis system to show FCD [30].

The mathematical model was challenged with ligand step changes which elicited the greatest cell response experimentally, namely 100 μM to 20 μM and 20 μM to 4 μM. For FCD to occur, each

signalling protein must react with an identical response curve to each of these five-fold changes, ie the CheY6-P response curves must be identical to each other, as must the CheY3-P curves etc. As can be seen in figure 4 each phosphorylated protein responds in an identical way to the two five-fold drops as their response curves superimpose exactly. These results, along with those discussed in Hamadeh *et al*. [30], confirm the *R. sphaeroides* signalling cascade can exhibit FCD. Interestingly, the shape of the adaptation curves for the various proteins are different. Experimentally, CheY6-P has been shown to be responsible for stopping the flagellar motor [23], whilst CheY3-P and CheY4-P also bind the motor but may modulate the effect of CheY6-P. We noted that the levels of the motor stopping CheY6-P quickly reached a saturating level during each fold change, whilst all the remaining protein levels did not. This result can be explained as follows. Because CheY6 is in high concentration throughout the cell and its phosphorylation is dominated by the transfer from CheA3-P rather than CheA2-P (see table S1 of the Supplementary Information), any variation in CheA3-P levels are mirrored by CheY6-P; the phosphotransfer occurs over a much shorter timescale than that of adaptation and thus saturating levels of CheY6-P are observed. In contrast the concentration of CheY3, CheY4, CheB1 and CheB2 is considerably less than that of CheY6. Furthermore, with the exception of phosphotransfer between CheA2-P and CheY4, and CheA2-P and CheB1, all the remaining phosphotransfer rates are considerably slower than that of CheA3-P to CheY6. Thus we expect the time taken for CheY3-P, CheY4-P, CheB1-P and CheB2-P to reach saturation levels to be considerably slower such that it may not occur during the adaptation time period. As CheY6-P is the major output causing the motor to stop [23], having this rapid transition between low and high concentrations may provide for a rapid physiological output in the chemotaxis response whilst other proteins follow a more graded transition, consistent with their having a role in the adaptation process or a more subtle modulation of the motor output.

3.4. Population adaptation times to different stimuli

We also challenged the model with 2- and 10-fold changes in attractant concentrations (figure 5), to identify how the phosphorylation levels of the constituent proteins was affected by the magnitude of the input. The time for the model to adapt was measured as the time taken for the major motor stopping CheY6-P levels to return to their prestimulus levels. Interestingly, the 2-fold change showed a response in the model with a short adaptation time of c. 25 seconds, compared with c. 45 seconds for the 5-fold change and 55 seconds for the 10-fold change. When the model was tested against our experimental data it was found that only a low percentage of cells show responses to a 2-fold change (figure 1*b*), probably due to the intrinsic cell to cell variations observed combined with the limit of time resolution for stop detection in our experimental setup. However, cells challenged with 10-fold changes in propionate concentration for background concentrations between 1mM and 10 μM showed adaptations times which were not longer for the 10-fold changes than for the 5-fold changes (figure 6). This is consistent with the relatively small increase in adaptation times suggested by the model (figure 5) being similar to the underlying intrinsic variation shown by the *R. sphaeroides* cell populations (figure 3*a*). Thus, the adaptation times do not appear to increase linearly with the magnitude of the fold change.

4. DISCUSSION

In this study we have investigated whether the output of the bacterial chemosensory pathway is altered by increased network complexity, protein expression levels or cellular architecture

compared to the simple well studied pathway of *E. coli*. Chemosensory responses were studied for *R. sphaeroides* cells grown either photosynthetically or aerobically i.e. in conditions in which cells have different cell architecture and chemosensory protein expression profiles [27,28,29].

Our results show that *R. sphaeroides* is sensitive to step changes in propionate concentration ranging over five to six orders of magnitude depending on the growth conditions (from 10 nM to about 10 mM). In this respect, *R. sphaeroides* is similar to *E. coli* which senses differences in attractant concentration over five to six orders of magnitude [10,16,17]. Therefore, despite significant differences in their chemotaxis pathways, the range and sensitivity over which *R. sphaeroides* is chemotactic is similar to that described for *E. coli* [10,16,17]. Interestingly, whilst all responsive cells behave similarly to a given stimulus regardless of growth conditions, photosynthetic populations of *R. sphaeroides* show a lower general percentage of cells responding to a given stimulus and the response of these cells saturate at high input concentrations earlier than cells in the aerobic populations. The reason for this is not currently known, but may reflect the lower average copy number of chemotaxis proteins expressed under photosynthetic growth conditions [28,29] and possibly the lower number of chemoreceptors [41] may become saturated by high levels of attractant.

In vivo FRET measurements, between the single CheY-P and its phosphatase CheZ, were used in *E. coli* to measure the entire shape of the chemosensory response (amplitude, adaptation time and precision) from a population of cells and to give a measure of the intracellular kinetics of the response and demonstrate FCD [19]. This is not possible in *R. sphaeroides* because it lacks a CheZ and it would be necessary to simultaneously measure the FRET interactions between three CheY proteins and two CheAs in this more complex signalling pathway, which is currently not technically possible. Therefore, we used a tethering assay to accurately quantify the whole input:output response as measured by the adaptation times of individual cells to different stimuli.

Our experimental results show that, irrespective of the growth conditions, individual *R. sphaeroides* cells display constant adaptation times to fold changes in concentration conforming to Weber's law and consistent with FCD for the entire signalling system. We then applied mathematical ODE based modelling to characterise the concentrations of the major intracellular signalling proteins during responses to different 5-fold drops in attractant concentration, as these are not directly measurable experimentally, and found that the model supported FCD in the *R. sphaeroides* chemotaxis pathway. Therefore, although we cannot experimentally measure response amplitudes, our data are consistent with the hypothesis that the *R. sphaeroides* chemosensory system shows Fold-Change Detection as recently demonstrated for the simpler pathway in *E. coli* [19]. Significantly, our results suggest that FCD occurs over similar background concentrations to the ones described in *E. coli* for methyl-aspartate [19], suggesting that neither the complexity of the chemosensory network in *R. sphaeroides* nor differences in cell architecture or protein expression profiles under different growth conditions influence FCD. This is also shown in the work of Hamadeh *et al.* [30] and supports the proposal that FCD could be a general feature of many biological sensory systems as hypothesized by Shoval and colleagues [20].

Analysis of the chemosensory responses of individual cells highlights that there is significant variability between cells in a genetically identical population, similar to observations/predictions made in *Salmonella enterica* S.v. Typhimurium [34] and *E. coli* [10,35,36]. Even though the majority of aerobic and photosynthetic cells show similar sensitivity and sensing features, a small proportion of cells can demonstrate higher sensitivity or different sensing properties by reacting to lower fold-changes. In addition, for both aerobic and photosynthetic cells, adaptation times were shown to vary both from cell-to-cell and when an individual cell was repeatedly challenged with the same stimulus. Phenotypic variability in adaptation times and in responsiveness to

chemoattractants could allow isogenic *R. sphaeroides* populations to optimise their search for nutrients and could represent a bet-hedging strategy to maximize survival.

The similarity in the chemotaxis responses of both aerobically and photoheterotrophically grown cells to each other, and to those previously determined for *E. coli*, suggests that general physiological features of chemotaxis may be a necessary consequence of their function. Our experimental data and modelling results, supported by the work of Hamadeh et al [30], suggest that the range and sensitivity of chemoattractant detection, adaptation times, adherence to Weber's law and Fold-Change Detection may be integral features of many chemotaxis systems, regardless of differences in network complexity, chemosensory protein expression profiles and cell architecture in different bacterial species.

ACKNOWLEDGMENTS

We are grateful to Kathryn Scott, David Wilkinson, Elaine Byles and Sonja Pawelczyk for their help with experiment preparation. This research was funded by the UK Biotechnology and Biological Sciences Research Council. MJT was funded by a Research Council UK Research Fellowship during the period this work was undertaken.

REFERENCES

[1] Berg, H.C. and Brown, D.A. 1972 Chemotaxis in *Escherichia coli* analysed by three-dimensional tracking. *Nature* **239:** 500–504.

[2] Segall, J.E., Block, S.M., and Berg, H.C. 1986 Temporal comparisons in bacterial chemotaxis. *Proc. Natl. Acad. Sci. USA* **83:** 8987–8991.

[3] Greer-Phillips, S.E., Stephens, B.B., and Alexandre, G. 2004 An energy taxis transducer promotes root colonization by *Azospirillum brasilense*. *J. Bacteriol.* **186**: 6595–6604.

[4] Miller, L.D., Yost, C.K., Hynes, M.F., and Alexandre, G. 2007 The major chemotaxis gene cluster of *Rhizobium leguminosarum* bv. viciae is essential for competitive nodulation. *Mol. Microbiol.* **63**: 348–362.

[5] Millikan, D.S. and Ruby, E.G. 2003 FlrA, a sigma54-dependent transcriptional activator in *Vibrio fischeri*, is required for motility and symbiotic light-organ colonization. *J. Bacteriol.* **185**: 3547–3557.

[6] Stoodley, P., Sauer, K., Davies, D.G., and Costerton, J.W. 2002 Biofilms as complex differentiated communities. *Annu. Rev. Microbiol.* **56**: 187–209.

[7] Garvis, S., Munder, A., Ball, G., de Bentzmann, S., Wiehlmann, L., Ewbank, J.J., *et al.* 2009 *Caenorhabditis elegans* semi-automated liquid screen reveals a specialized role for the chemotaxis gene cheb2 in *Pseudomonas aeruginosa* virulence. *PLoS Pathog.* **5**: e1000540.

[8] Williams, S.M., Chen, Y.T., Andermann, T.M., Carter, J.E., McGee, D.J., and Ottemann, K.M. 2007 *Helicobacter pylori* chemotaxis modulates inflammation and bacterium-gastric epithelium interactions in infected mice. *Infect. Immun.* **75**: 3747–3757.

[9] Wadhams, G.H. and Armitage, J.P. 2004 Making sense of it all: bacterial chemotaxis. *Nat. Rev. Mol. Cell Biol.* **5**: 1024–1037.

[10] Berg, H.C. and Tedesco, P.M. 1975 Transient response to chemotactic stimuli in *Escherichia coli*. *Proc. Natl. Acad. Sci. USA* **72**: 3235–3239.

[11] Turner, L., Ryu, W.S., and Berg, H.C. 2000 Real-time imaging of fluorescent flagellar filaments. *J. Bacteriol.* **182**: 2793–2801.

[12] Baker, M.D., Wolanin, P.M., and Stock, J.B. 2006 Signal transduction in bacterial chemotaxis. *Bioessays* **28**: 9–22.

[13] Eisenbach, M. 2007 A hitchhiker's guide through advances and conceptual changes in chemotaxis. *J. Cell Physiol.* **213**: 574–580.

[14] Hazelbauer, G.L., Falke, J.J., and Parkinson, J.S. 2008 Bacterial chemoreceptors: high-performance signaling in networked arrays. *Trends Biochem. Sci.* **33**: 9–19.

[15] Mao, H., Cremer, P.S., and Manson, M.D. 2003 A sensitive, versatile microfluidic assay for bacterial chemotaxis. *Proc. Natl. Acad. Sci. USA* **100**: 5449–5454.

[16] Mesibov, R., Ordal, G.W., and Adler, J. 1973 The range of attractant concentrations for bacterial chemotaxis and the threshold and size of response over this range. Weber law and related phenomena. *J. Gen. Physiol.* **62**: 203–223.

[17] Neumann, S., Hansen, C.H., Wingreen, N.S., and Sourjik, V. 2010 Differences in signalling by directly and indirectly binding ligands in bacterial chemotaxis. *EMBO J.* **29**: 3484–3495.

[18] Kalinin, Y., Neumann, S., Sourjik, V., and Wu, M. 2010 Responses of *Escherichia coli* bacteria to two opposing chemoattractant gradients depend on the chemoreceptor ratio. *J. Bacteriol.* **192**: 1796–1800.

[19] Lazova, M.D., Ahmed, T., Bellomo, D., Stocker, R., and Shimizu, T.S. 2011 Response rescaling in bacterial chemotaxis. *Proc. Natl. Acad. Sci. USA* **108:**13870-13875.

[20] Shoval, O., Goentoro, L., Hart, Y., Mayo, A., Sontag, E., and Alon, U. 2010 Fold-change detection and scalar symmetry of sensory input fields. *Proc. Natl. Acad. Sci. USA* **107**: 15995–

16000.

[21] Mackenzie, C., Eraso, J.M., Choudhary, M., Roh, J.H., Zeng, X., Bruscella, P., *et al.* 2007 Postgenomic adventures with *Rhodobacter sphaeroides*. *Annu. Rev. Microbiol.* **61**: 283–307.

[22] Porter, S.L., Wadhams, G.H., and Armitage, J.P. 2008 *Rhodobacter sphaeroides*: complexity in chemotactic signalling. *Trends Microbiol.* **16**: 251–260.

[23] Porter, S.L., Wadhams, G.H., and Armitage, J.P. 2011 Signal processing in complex chemotaxis pathways. *Nat. Rev. Microbiol.* **9:** 153-165.

[24] Hamblin, P.A., Maguire, B.A., Grishanin, R.N., and Armitage, J.P. 1997 Evidence for two chemosensory pathways in *Rhodobacter sphaeroides*. *Mol. Microbiol.* **26**: 1083–1096.

[25] Porter, S.L., Warren, A.V., Martin, A.C., and Armitage, J.P. 2002 The third chemotaxis locus of *Rhodobacter sphaeroides* is essential for chemotaxis. *Mol. Microbiol.* **46**: 1081–1094.

[26] Romagnoli, S., Packer, H.L., and Armitage, J.P. 2002 Tactic responses to oxygen in the phototrophic bacterium *Rhodobacter sphaeroides* WS8N. *J. Bacteriol.* **184**: 5590–5598.

[27] Tucker, J.D., Siebert, C.A., Escalante, M., Adams, P.G., Olsen, J.D., Otto, C., *et al.* 2010 Membrane invagination in *Rhodobacter sphaeroides* is initiated at curved regions of the cytoplasmic membrane, then forms both budded and fully detached spherical vesicles. *Mol. Microbiol.* **76**: 833–847.

[28] Shah, D.S., Porter, S.L., Martin, A.C., Hamblin, P.A., and Armitage, J.P. 2000 Fine tuning bacterial chemotaxis: analysis of *Rhodobacter sphaeroides* behaviour under aerobic and anaerobic conditions by mutation of the major chemotaxis operons and *chey* genes. *EMBO J.* **19**: 4601–4613.

[29] Roh, J.H., Smith, W.E., and Kaplan, S. 2004 Effects of oxygen and light intensity on transcriptome expression in *Rhodobacter sphaeroides* 2.4.1. redox active gene expression profile. *J. Biol. Chem.* **279**: 9146–9155.

[30] Hamadeh, A., Ingalls, B. and Sontag, E. 2012 Transient dynamic phenotypes as criteria for model discrimination: fold-change detection in *Rhodobacter sphaeroides* chemotaxis. Submitted *J. Roy. Soc. Interf.*

[31] Sockett, R.E., Foster, J.C.A., and Armitage, J.P. 1990 Molecular biology of the *Rhodobacter sphaeroides* flagellum. *FEMS Symp.* **53**: 473–479.

[32] Sistrom, W.R. 1960 A requirement for sodium in the growth of *Rhodopseudomonas spheroides*. *J. Gen. Microbiol.* **22**: 778–785.

[33] Kojadinovic, M., Sirinelli, A., Wadhams, G.H., and Armitage, J.P. 2011 New motion analysis system for characterization of the chemosensory response kinetics of *Rhodobacter sphaeroides* under different growth conditions. *Appl. Environ. Microbiol.* **77:** 4082–4088.

[34] Spudich, J.L. and Koshland, D.E. 1976 Non-genetic individuality: chance in the single cell. *Nature* **262**: 467–471.

[35] Korobkova, E., Emonet, T., Vilar, J.M.G., Shimizu, T.S., and Cluzel, P. 2004 From molecular noise to behavioural variability in a single bacterium. *Nature* **428**: 574–578.

[36] Meir, Y., Jakovljevic, V., Oleksiuk, O., Sourjik, V., and Wingreen, N.S. 2010 Precision and kinetics of adaptation in bacterial chemotaxis. *Biophys. J.* **99**: 2766–2774.

[37] Tindall, M.J., Porter, S.L., Maini, P.K. and Armitage, J.P 2010 Modeling chemotaxis reveals the role of reversed phosphotransfer and a bi-functional kinase-phosphatase. *PLoS Comput. Biol.* **6 :** e100896.

[38] Endres, R.G. and Wingreen, N.S. 2006 Precise adaptation in bacterial chemotaxis through ``assistance neighbourhoods''. *Proc. Nat. Acad. Sci. USA* **103:** 13040-13044.

[39] Clausznitzer, D., Oleksiuk, O., Lovdok, L., Sourjik, V. and Endres, R.G. 2010 Chemotactic response and adaptation dynamics in *Escherichia coli*. *PLoS Comput. Biol*. **6:** e1000784, 2010.

[40] Tu, Y, Shimizu, T.S. and Berg, H.C. 2008 Modeling the chemotactic response of

Escherichia coli to time-varying stimuli. *Proc. Natl. Acad. Sci. USA* **105**: 14855-60.

[41] Harrison, D.M., Skidmore, J., Armitage, J.P., and Maddock, J.R. 1999 Localization and environmental regulation of Mcp-like proteins in *Rhodobacter sphaeroides*. *Mol. Microbiol.* **31**: 885–892.

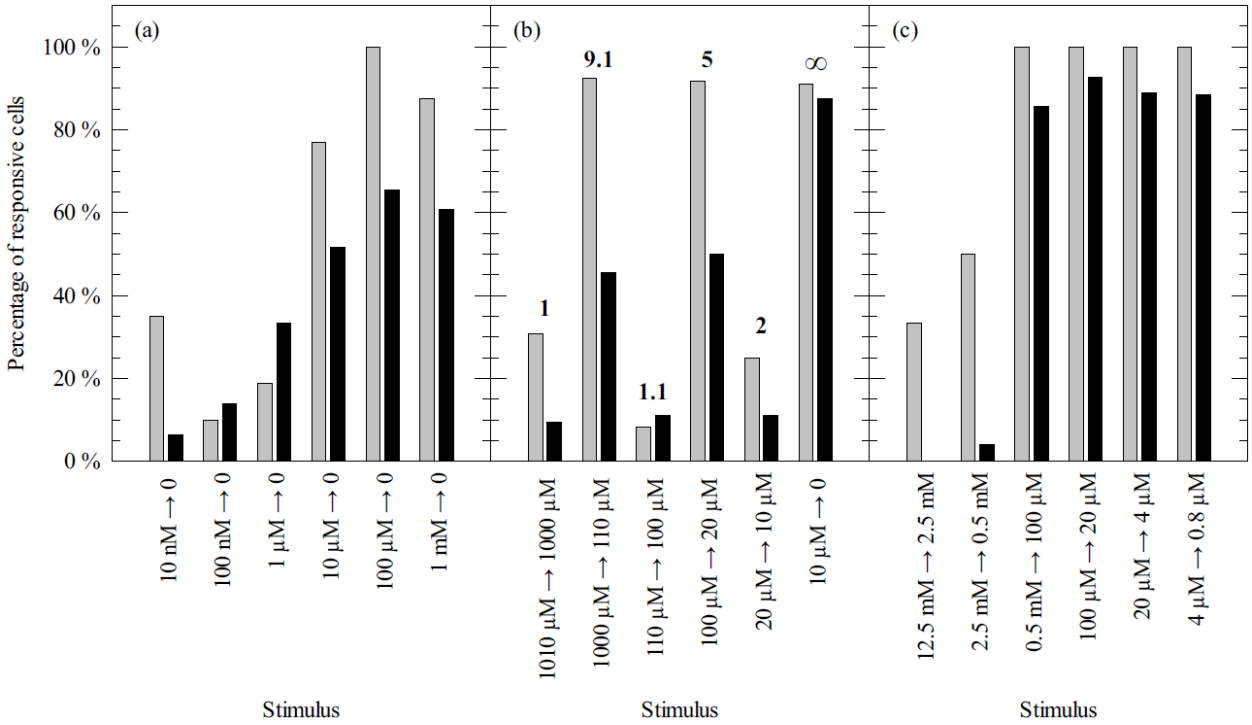

Figure 1. Percentages of aerobic (grey bars) and photosynthetic (black bars) cells from each population that are responsive to different step drops in propionate concentration. (a): Percentages of cells responsive to increasing step drops to zero (i.e. to tethering buffer). The number of cells analyzed for each drop in concentration was between 23 and 36 for photosynthetically grown cells and 8 and 20 for aerobically grown cells. (b): Percentages of cells responsive to 10 µM drops in propionate concentration over different background concentrations. The number of cells analyzed for each stimulus was between 8 and 22 for photosynthetically grown cells and 11 and 13 for aerobically grown cells. Numbers above the bars represent the fold-change in concentration for each stimulus. (c): Percentages of cells responsive to different 5-fold drops in propionate concentration. The number of cells analyzed for each stimulus was between 19 and 26 for photosynthetic cells and between 21 and 23 for aerobic cells.

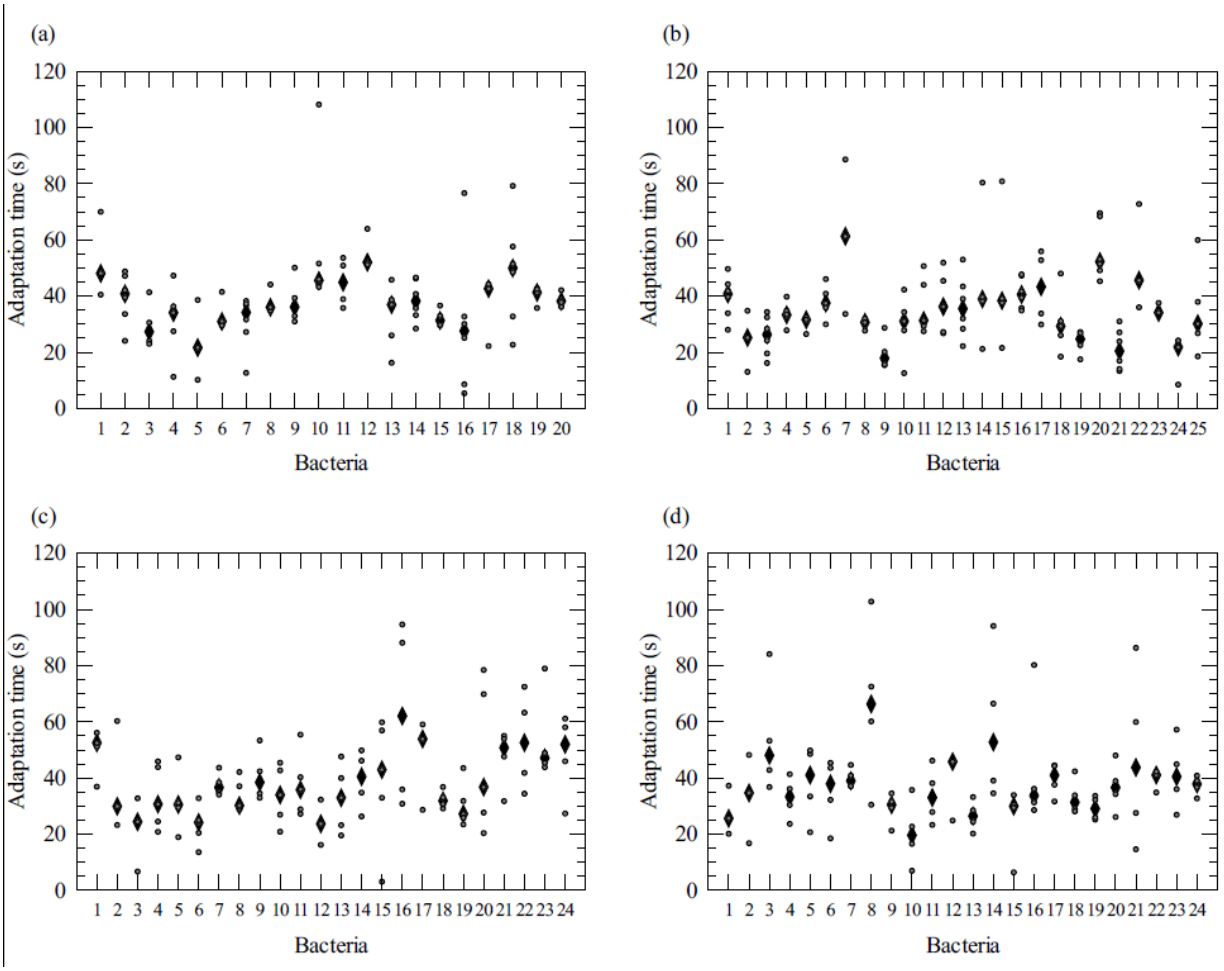

Figure 2. Adaptation times of responsive single-cells to 5 fold-drops in propionate concentrations. (a), (c): Aerobic single-cell adaptation times. (b), (d): Photosynthetic single-cell adaptation times. (a), (b): Adaptation times to six successive drops from 100 µM to 20 µM in propionate concentration. (c), (d): Adaptation times to different 5-fold drops in propionate concentration. Lozenges represent the median adaptation time of a single-cell. The circles represent responses of a single-cell to successive stimuli. Only cells responding to at least three stimuli are represented.

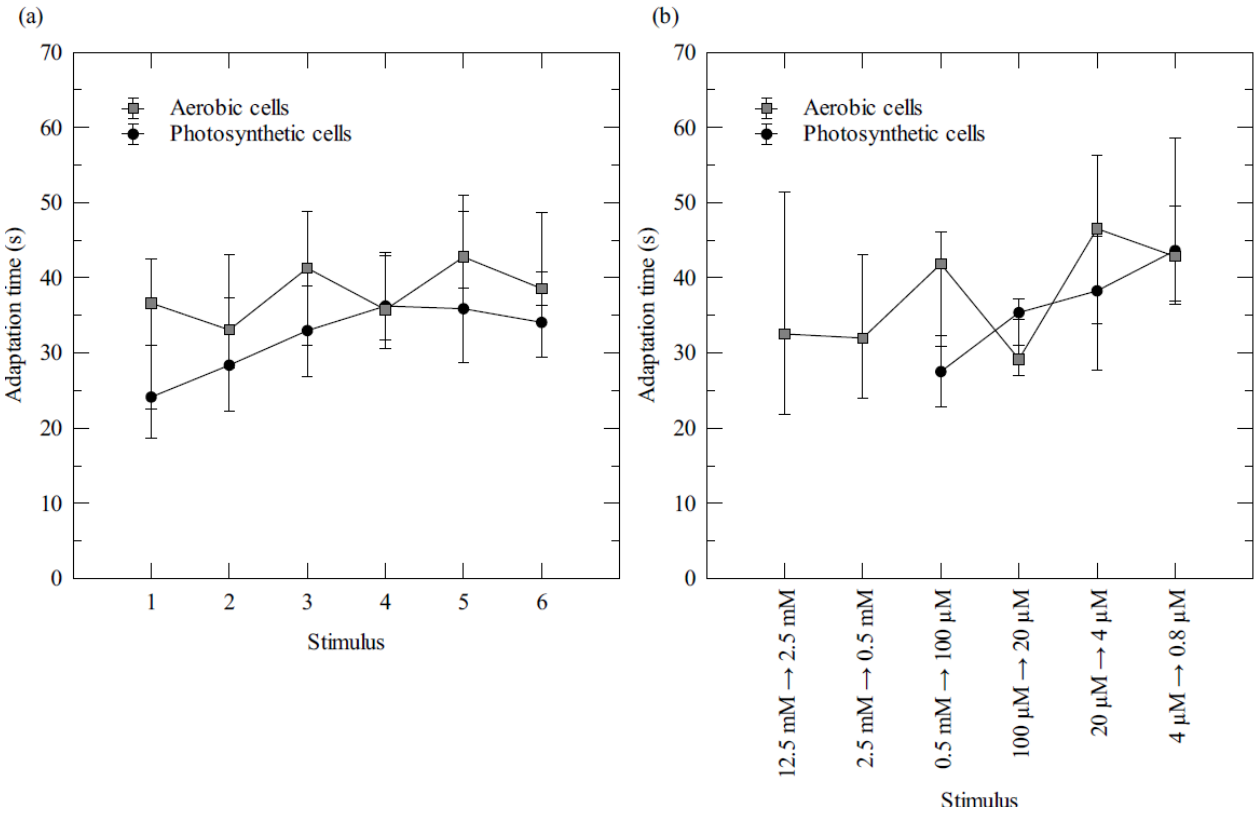

Figure 3. Adaptation times of responsive cell populations to 5-fold drops in propionate concentrations. (a): Responses to six drops in concentration from 100 µM to 20 µM. (b): Responses to 5-fold drops over different background concentrations. The number of cells analyzed for each drop in concentration was between: (a) 26 and 20 for photosynthetic cells and 12 and 22 for aerobic cells, (b) 23 and 24 for photosynthetic cells and 6 and 25 for aerobic cells. Only data sets comprised of more than 3 cells are represented. Symbols represent data medians. The lower and the upper limits of the bars represent the first and the third quartiles of the data respectively.

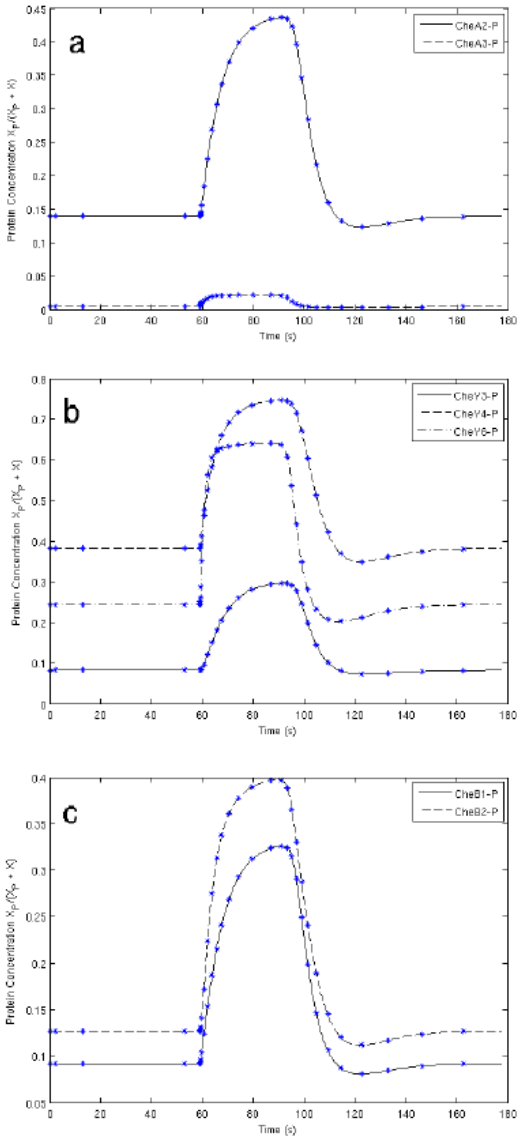

Figure 4. Model results showing FCD in *R. sphaeroides* for: (a) the kinases CheA2-P and CheA3-P; (b) the response regulator proteins CheY3-P, CheY4-P, CheY6-P; and (c) the adaptation proteins CheB1-P and CheB2-P. 5-fold variations in the attractant ligand concentration were considered; Case 1 (line) : 100 μM to 20 μM and Case 2 (symbols): 20 μM to 4 μM. Each variation in protein concentration for Case 1 and Case 2 overlies the other. Here the amount of each phosphorylated protein has been scaled against its total amount of protein (the sum of its phosphorylated and unphosphorylated states).

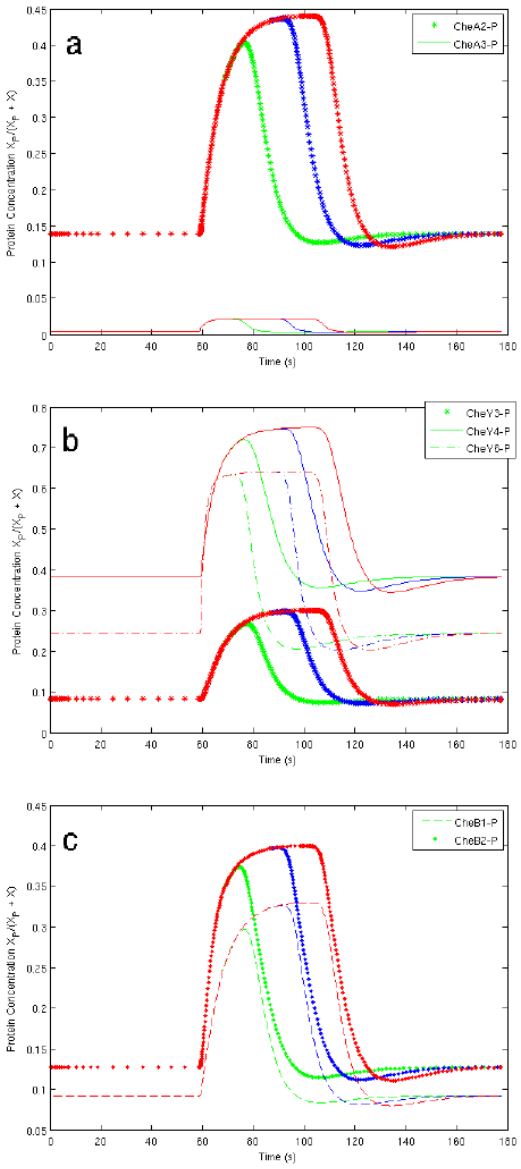

Figure 5. Variation in adaptation time for the mathematical model challenged with 2-fold (100 μM to 50 μM), 5-fold (100 μM to 20 μM) and 10-fold (100 μM to 10 μM) ligand step changes for: (a) CheA2-P and CheA3-P; (b) CheY3-P, CheY4-P and CheY6-P; and (c) CheB1-P and CheB2-P. 2-fold changes are marked in green, 5-fold in blue and 10-fold in red. Here the amount of each phosphorylated protein has been scaled against its total amount of protein (the sum of its phosphorylated and unphosphorylated states).

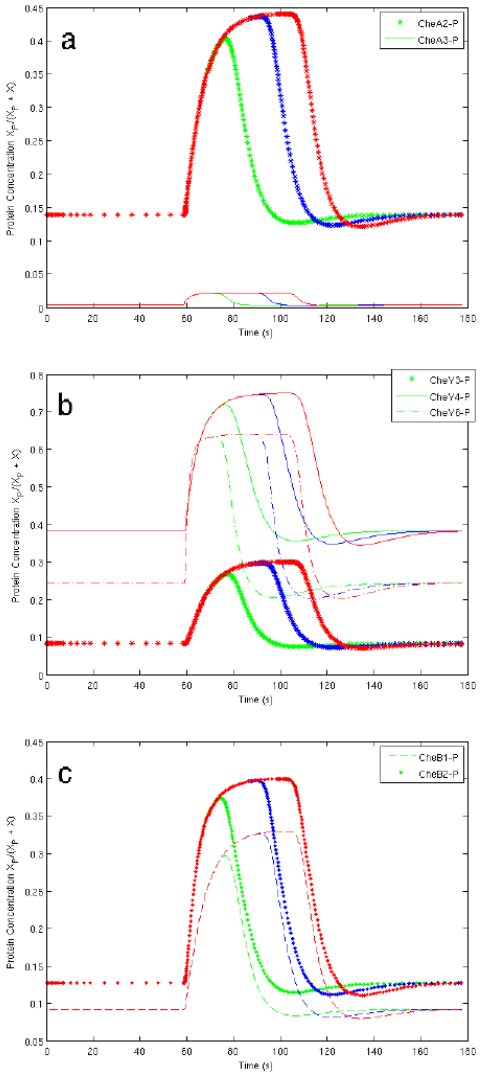

Figure 6. Adaptation times of responsive cell populations to 5-fold changes (in black) and 10-fold changes (in white). Circles represent median responses of photosynthetic cell populations and squares median responses of aerobic cell populations. The number of cells analyzed for each drop in concentration was between, for 5 fold-changes: 23 and 25 for photosynthetic cells and 6 and 25 for aerobic cells; for 10-fold changes: 4 and 18 for photosynthetic cells and 3 and 12 for aerobic cells. Only data sets comprised of more than 3 cells are represented. The lower and the upper limits of the bars represent the first and the third quartiles of the data respectively.